Monte Carlo Simulation of extreme traffic loading on short and medium span bridges

Bernard Enright[1] and Eugene J. OBrien[2]

[1] Dublin Institute of Technology, Ireland

[2] University College Dublin, Ireland

ABSTRACT

The accurate estimation of site-specific lifetime extreme traffic load effects is an important element in the cost-effective assessment of bridges. A common approach is to use statistical distributions derived from weigh-in-motion (WIM) measurements as the basis for Monte Carlo simulation of traffic loading over a number of years, and to estimate lifetime bridge load effects by extrapolation from the results of this simulation. However, results are sensitive to the assumptions made, not just with regard to vehicle weights but also to number of axles, inter-axle spacings and gaps between vehicles. This paper carries out a critical review of the assumptions involved in the process. It presents a comprehensive model for Monte Carlo simulation of bridge loading for free-flowing traffic that can be applied to different sites, and shows how the model matches results obtained from extensive sets of WIM measurements for highway sites in five European countries. The model allows for the simulation of vehicles which are heavier and have more axles than those recorded in the WIM data, and uses techniques for modeling axle configuration that can be applied to any type of vehicle. The model presented in this paper has been optimized to allow the simulation of 1000 or more years of traffic and this greatly reduces the variance in the process of calculating estimates for lifetime loading from the simulation model. Using this approach, it is possible to analyze the type of loading scenarios that cause the maximum lifetime load effects. Conclusions can be drawn about the type of vehicles likely to be involved in maximum lifetime loading scenarios, and the results highlight the importance of special vehicles in bridge loading. The approach described here does not remove the uncertainty inherent in estimating lifetime maximum loading from data collected over time periods which are much shorter than the bridge lifetime.

Keywords: Bridge, assessment, weigh-in-motion, Monte Carlo simulation, traffic loading, special vehicles

1. INTRODUCTION

In recent years, the improved quality and increasing use of weigh-in-motion (WIM) technology [1] has meant that more accurate measurements of vehicle weights are now available for periods covering many months or even years of traffic at selected locations. These extensive measurements can be used to refine probabilistic bridge loading models for the assessment of existing bridges, and to monitor the implications for bridge design of trends in vehicle weights and types. Codes of practice for the design of bridges such as the Eurocode [2] must be sufficiently general to be applicable to many different bridge types with widely varying traffic loading conditions [3,4]. Assessment codes are also general, and in many cases may be conservative [5] despite the fact that bridge maintenance is expensive, and bridge owners need to allocate limited resources efficiently. Site-specific assessment, based on measured traffic, can lead to very significant cost reductions for maintenance [6], and the application of site-specific models for bridge assessment has been widely studied [5,7-9].

European and North American codes are based on relatively small amounts of data collected some years ago. The U.S. and Canadian codes are based on data collected in Ontario in 1975 for 9250 trucks [10,11]. The Eurocode [2] was initially based on a number of weeks of data from Auxerre in the 1980s [3,12], and was confirmed using data from a number of French sites in 1997 [13]. Changing truck weights [14], composition of traffic, and vehicle sizes all have implications for bridge loading, and codes need to be periodically re-calibrated based on current traffic. This study is based on WIM data collected between 2005 and 2008 for 2.7 million trucks at five European sites – in the Netherlands, Slovakia, the Czech Republic, Slovenia and Poland. Codes segregate normal legal traffic (with some allowance for illegal overloading) from special vehicles which require permits [2,15]. Special vehicles are very important for bridge loading [5,16], and the model developed for this study seeks to include all vehicles, normal and special, that are likely to cross a bridge at full highway speed during its lifetime.

It is necessary to estimate as accurately as possible the probable maximum bridge load effects (bending moments, shears) over a selected lifetime. For assessment, this can be 5 to 10 years [17], whereas for design the U.S. AASHTO code is based on the distribution of the 75-year maximum loading [10]. The Eurocode [2] for the design of new bridges is based on the distribution of the 50-year maximum, and the characteristic load is calculated as the value with a 5% probability of being

exceeded in the 50 year lifetime, which is approximately equivalent to the value with a return period of 1000 years. Even with the relatively large amounts of truck data gathered for this study, it is still necessary to extrapolate from the measured data to calculate estimates of lifetime maximum bridge loading. This is true regardless of the particular method adopted. One approach is to fit a statistical distribution to the calculated load effects for the measured traffic, and to use these distributions to estimate characteristic lifetime maximum effects [10,18,19]. An alternative approach adopted by many authors is to use Monte Carlo (MC) simulation [20-22], and this is the approach adopted here.

In the development of the U.S. AASHTO code for bridge design [10], load effects were calculated for the measured trucks on different bridge spans and plotted on Normal probability paper. The curves were extrapolated to give estimates for the mean 75-year load effect, and the coefficient of variation was estimated by raising the distributions to a power based on typical truck volumes. This process requires a significant degree of engineering judgment and subjectivity, as noted by Kulicki [4], Miao and Chan [19] and by Gindy and Nassif [23] who report variations in estimated lifetime maxima of up to 33%. In the development of the Eurocode [2], traffic measurements were collected over some weeks at different times, and a number of different extrapolation techniques were applied. Multimodal Normal and Gumbel distributions were fitted to measured load effects for individual loading events, and the Gumbel extreme value distribution was fitted to periodic maxima calculated from simulation. Dawe [12] reports variations of up to 20% between results from the different approaches used in the development of the Eurocode.

In the Monte Carlo simulation approach, statistical distributions for vehicle weights, inter-vehicle gaps and other characteristics are derived from the measurements, and are used as the basis for the simulation of traffic, typically for some number of years. It is thus possible to simulate vehicles and combinations of vehicles that have not been observed during the period of measurement. Lifetime maximum load effects have usually been estimated by extrapolating from the results of the simulation. Cooper [24] uses the Gumbel extreme value distribution for extrapolation, whereas the Generalized Extreme Value (GEV) distribution is applied by Caprani et al. [25] for simulations of up to five years of traffic, and by James [26] who notes its sensitivity to changes in the shape parameter. The GEV distribution incorporates the Gumbel, Fréchet (unbounded) and Weibull (bounded) distributions. Fitting a distribution to the full data set of periodic maxima can give

excessive emphasis to loading scenarios which do not make any significant contribution to the characteristic value. Castillo [27] recommends fitting the Gumbel distribution to the upper tail of the data (by selecting the top $2\sqrt{n}$ data points), but this risks placing excessive emphasis on a small number of extreme cases. Crespo-Minguillón and Casas [28] and James [26] use the peaks over threshold extreme value approach, while Cremona [29] adopts the Rice level-crossing technique. In this paper, the MC model has been optimized to make it practical to simulate thousands of years on a conventional desktop computer, and if the simulation is run for a sufficiently long time, the lifetime maximum load effects can be found directly from the results of the simulation. Running the simulation for 1000 years and fitting a distribution for smoothing purposes is more efficient than simulating many thousands of years, and is found to give sufficiently good estimates. Using long-run simulations avoids the problems of extrapolating from short simulation runs, and gives much more consistent results compared with existing MC simulation approaches.

In order to simplify the simulation process, various restrictions are often placed on the traffic model used – some authors specify a maximum value for vehicle weights, and many use a limited set of vehicle classes with a fixed maximum number of axles [20,30-32]. Some employ limited modeling of inter-vehicle gaps [10,18,30]. Vehicle models are typically based on existing vehicle types only, without attempting to extrapolate for vehicle types other than those recorded [24]. The approach used here is to build a detailed MC model, without any restrictive assumptions, and to calibrate it against extensive WIM data collected at five European sites. The model is designed to extrapolate both vehicle weights and types (axle configurations), and while this extrapolation is based on assumptions which will influence the results, it is considered to give a more realistic estimate of lifetime loading than previous MC models.

Estimating lifetime loading from short periods of measured or simulated data does not give a clear idea of what types of trucks are likely to be involved in lifetime maximum loading events. Long-run simulations provide examples of the types and combinations of vehicles that might be expected to feature in extreme bridge loading. This is useful in identifying the relative importance of factors such as gross vehicle weight (GVW), the weights of individual axles and of groups of axles, wheelbase, and axle layout. This in turn may help in identifying useful legal restrictions on truck types. Simulating 1000 years or more of traffic also makes it possible to model extremely rare events such as one exceptionally heavy truck or a number of extremely heavy trucks meeting on a

bridge which can be critical in its lifetime [5]. Identification of such rare events is a potential problem with short-run simulations [33].

This study focuses on free-flowing, rather than congested, traffic on short to medium span bridges. In the range of spans considered, from 15 to 45 m, the combination of static and dynamic load effects produced by free-flowing traffic is assumed to govern bridge loading. In longer spans, static loading produced by congested traffic is generally considered to be more critical [3].

2. DESCRIPTION OF WIM DATA

A large database of WIM measurements was collected for trucks weighing 3.5 t or more at five European sites between 2005 and 2008, as detailed in Table 1. The recorded data were cleaned to remove unreliable observations. This cleaning is essential in identifying and removing incorrect vehicle data that would otherwise distort the subsequent analysis [9]. Cameras at the WIM site in the Netherlands proved very useful in the formulation of rules for data cleaning at all sites. Between all sites, an average of 1.5% of recorded vehicles was removed as a result of data cleaning. For accurate modeling of very small inter-vehicle gaps, a precision of 0.01 seconds or better is preferable when recording vehicle arrival times; although a lower precision of 0.1 seconds is still acceptable. At the site in Poland, the precision of 1 second makes it difficult to calibrate the simulation model for small inter-vehicle gaps.

It can be seen that some extremely heavy vehicles were recorded, with the maximum GVW at each site being in excess of 100 t. The GVW histograms for two of the sites are illustrated in Fig. 1. The distribution of weights up to 70 t shown in Fig. 1(a) is typical of heavily trafficked European highways [20-22,32]. Significant numbers of very heavy vehicles were also recorded at both sites, as can be seen in Fig. 1(b). The site in the Netherlands has a much higher proportion of very heavy vehicles, with 892 vehicles whose GVW is in excess 70 t and 236 vehicles in excess of 100 t, up to the heaviest observed GVW of 165.6 t. The corresponding figures for the site in Slovakia are 78 vehicles in excess of 70 t, 8 vehicles in excess of 100 t, and a maximum observed GVW of 117.1 t. Almost all of the very heavy vehicles at the site in the Netherlands are in the slow lane, with just seven vehicles in excess of 70 t in the faster lane, and a maximum there of 75.2 t.

Table 1. WIM data

Country	Netherlands (NL)	Slovakia (SK)	Czech Republic (CZ)	Slovenia (SI)	Poland (PL)
Site	Woerden	Branisko	Sedlice	Vransko	Wroclaw
Road number	A12 (E25/E30)	D1 (E50)	D1 (E50/E65)	A1 (E57)	A4 (E40)
Number of measured lanes	2	2	2	2	2
Number of directions	1	2	1	1	1
Total trucks (cleaned)	646 548	748 338	729 929	147 752	429 680
Time period	Feb to Jun 2005	Jun 2005 to Dec 2006	May 2007 to May 2008	Sep to Nov 2006	Jan to Jun 2008
Number of weekdays with full traffic record	77	290	148	39	87
Average daily truck traffic (ADTT) in one direction	7 102	1 100	4 751	3 293	4 022
Time stamp precision (s)	0.01	0.1	0.1	0.001	1.0
Maximum number of axles	13	11	12	12	9
Maximum GVW (t)	165.6	117.1	129.0	131.3	105.9
Number over 70 t	892	78	169	3	35

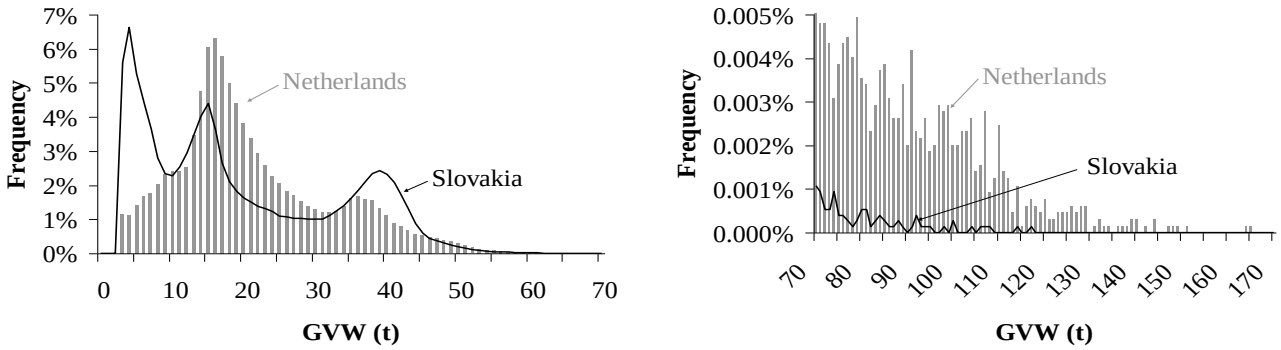

(a) Less than 70 t (b) In excess of 70 t

Fig. 1. GVW histograms for the Netherlands and Slovakia

3. SIMULATION METHODOLOGY

In Monte Carlo simulation, the parameters for each individual truck, and for the arrangement of trucks in each lane, are generated using lane-specific statistical distributions derived from the traffic

measured at each site. The calculated characteristic load effects are sensitive to the assumptions used for these distributions. Most simulated vehicles will be within the observed range of vehicle classes (number of axles), but the modeling of extreme vehicles with more axles than any observed is also necessary. The latter are described in Section 3.2.

3.1. Observed vehicle classes

Many models for GVW have been used by other authors. Bimodal and trimodal Normal distributions have been used for the entire truck population [21,34,35]. Others have focused on the weights of heavy trucks only – Kennedy et al. [36] assume that these can be described by a Normal distribution, whereas Grave et al. [32] model these with a Weibull distribution. Bailey and Bez [20] use a Beta distribution to model the weights of axle groups (tandems and tridems) and build up the GVW from this. Crespo-Minguillón and Casas [28] use the measured empirical distribution (bootstrapping) as the basis for MC simulation. Typically, the simulation is designed so that the proportion of vehicles in each class is the same as in the measured traffic. The vehicle class may be determined simply by the number of axles (and this is the approach adopted here), or in some studies further sub-classification is applied based on axle layout [20,22].

In this study, the GVW and number of axles for each truck are generated using the 'semi-parametric' approach developed by O'Brien et al. [37]. Up to a certain GVW threshold, where there are enough data to provide a clear frequency trend, an empirical bivariate distribution is used for GVW and number of axles. The threshold chosen for this is the value of GVW for which the bin count in the GVW histogram for all vehicles crosses 16 (using a bin size of 1 t). Beyond this threshold, a parametric fit is needed in order to smooth the trend and so that simulations can generate vehicles with weights and numbers of axles greater than those observed. The upper quadrant of a bivariate Normal distribution is fitted to the frequencies above the GVW threshold using truncated maximum likelihood estimation. The choice of the Normal distribution is not based on theoretical considerations, but it is widely used, fits the data reasonably well, and does not have an upper bound. The thresholds used, together with the expected 1000-year GVW (based on the fitted distribution), and the parameters of the bivariate Normal distribution are shown for each site in Table 2. Only the upper quadrant of the distribution is used, and the overall distribution does not have a physical meaning, as is evidenced by the negative mean values in some cases. As discussed

in O'Brien et al. [37], results for lifetime maximum loading vary to some degree based on decisions made about extrapolation of GVW, and these decisions are, of necessity, based on relatively sparse observed data.

Table 2. GVW and number of axles – Upper quadrant of bivariate Normal distribution (μ = mean; σ = standard deviation; ρ = correlation coefficient)

Site	**GVW Threshold (t)**	**Expected 1000-year GVW (t)**	μ_{GVW} **(t)**	σ_{GVW} **(t)**	μ_{NAxles}	σ_{NAxles}	ρ
Netherlands	100	234	64.9	27.9	7.2	2.1	0.82
Slovakia	64	167	11.3	26.2	2.9	2.2	0.79
Czech Republic	62	189	14.6	29.1	4.3	2.5	0.75
Slovenia	59	175	-61.3	42.4	-4.1	3.7	0.97
Poland	70	158	-3.9	28.2	1.0	2.2	0.92

The importance of wheelbase in bridge loading is well recognized. Sivakumar et al. [16] note that vehicles with closely-spaced axles such as specialized haulage vehicles – concrete trucks, construction vehicles – tend to govern bridge loading, and Tabsh and Tabatabai [38] discuss the importance of short-wheelbase vehicles in lateral distribution of loads. Design codes such as the Eurocode [2] incorporate some variation in axle spacing in load models for special vehicles, and in this study the accurate modeling of axle spacing is given close attention. Photographs from the Netherlands of heavy vehicles show that shorter special vehicles are frequently cranes or vehicles carrying crane ballast, as in Fig. 2(a), which often travel in convoy with cranes. These are characterized by a series of closely-spaced axles. Vehicles with a large maximum axle spacing are often "low loaders" carrying construction equipment, as in Fig. 2(b). These vehicles might be expected to have special permits and escort vehicles, but were recorded travelling at speeds similar to other traffic and are typically part of the general traffic on the highway. Different approaches have been used in the past to model axle spacing for each vehicle class – some have assumed fixed axle spacings [32,34]; Bailey and Bez [20] use Beta distributions for spacings; Sriramula et al. [39] use Normal distributions and model correlation between spacings using copula functions; O'Brien et al. [21] use a combination of unimodal and bimodal Normal distributions. In this study, for each vehicle measured, all axle spacings are ranked in descending order, starting with the maximum. In

the MC simulation, an empirical distribution (bootstrapping) is used to generate the maximum axle spacing for each vehicle, given the number of axles and the GVW range (in 5 t intervals). A sample illustrating this empirical distribution is given in Table 3. A lower limit of 1 m, and an upper limit of 20 m ensure that unrealistic axle spacings are not generated. For all spacings other than the maximum, fitted trimodal Normal distributions are used, as illustrated in Table 4. Axle spacings are assumed to be independent of each other. The density function for a trimodal Normal distribution is given by:

$$f(x) = p_1 N(\mu_1, \sigma_1) + p_2 N(\mu_2, \sigma_2) + p_3 N(\mu_3, \sigma_3) \quad (1)$$

where $N(\mu, \sigma)$ is the Normal density function with mean μ and standard deviation σ,

$0 \le p_i \le 1$ and $p_1 + p_2 + p_3 = 1$.

The *position* of each of the ranked spacings on the vehicle is also modeled in the simulation using empirical distributions for all spacings in each vehicle class, and a sample is shown in Table 5.

Table 3. Sample extract from empirical distribution: frequencies of maximum axle spacing/GVW combinations (6-axle trucks, Czech Republic)

Number of axles = 6											
	Maximum axle spacing (m)										
GVW (t)	1	2	3	4	5	6	7	8	9	10	…20
…											
20	0	0	36	318	397	127	21	29	21	5	
25	0	1	7	129	183	73	21	20	19	17	
30	0	0	11	73	167	56	34	20	12	35	
…											

Table 4. Parameters of sample trimodal Normal distributions for other axle spacings (6-axle trucks, Czech Republic)

Spacing	μ_1 (m)	σ_1 (m)	p_1	μ_2 (m)	σ_2 (m)	p_2	μ_3 (m)	σ_3 (m)	p_3
2nd Max	3.14	0.49	66%	4.57	0.24	30%	6.53	0.92	4%
3rd Max	1.39	0.05	57%	2.27	0.05	0%	3.53	0.86	43%
4th Max	1.37	0.34	7%	1.37	0.05	87%	2.63	0.92	6%
Smallest	1.26	0.05	16%	1.34	0.05	79%	1.34	0.69	5%

Table 5. Sample empirical distribution for positions of largest spacings (6-axle trucks, Czech Republic)

Position	1st Max	2nd Max	3rd Max	4th Max
1	13%	78%	7%	2%
2	5%	5%	24%	38%
3	73%	13%	4%	5%
4	7%	3%	36%	23%
5	1%	1%	29%	33%

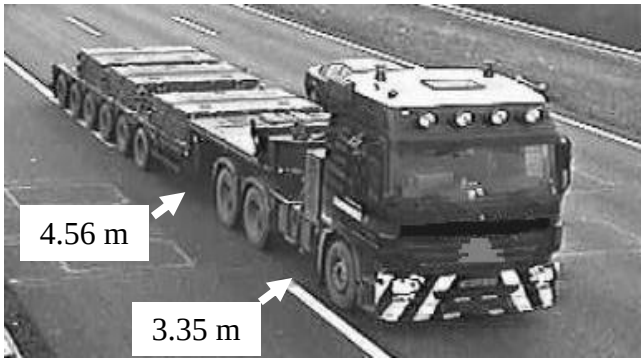

(a) GVW=100.1 t, wheelbase=16.2 m (carrying crane ballast).

(b) GVW=100.8 t, wheelbase=22.3 m

Fig. 2. Two 9-axle vehicles recorded in the Netherlands

The approach used is illustrated for the case of 9-axle vehicles recorded in the Netherlands, and two typical examples are shown in Fig. 2. The axle layout for the vehicle of Fig. 2(a) can be characterized as follows: it has a maximum spacing of 4.56 m behind the third axle, the next largest

spacing of 3.35 m behind the first axle, with all other spacings approximately 1.40 m. The vehicle of Fig. 2(b) has a maximum spacing of 11.04 m behind the fourth axle, the next largest spacing of 2.53 m is behind the first axle, with all other spacings between 1.30 and 1.50 m.

The distributions of the magnitude of the first and second largest spacings for all 9-axle trucks in the Dutch data are shown in Fig. 3(a), and a distinct bimodal shape for the maximum spacing is evident, corresponding to crane-type vehicles and low loaders. The distributions of the position of the first and second largest spacings are shown in Fig. 3(b) which shows that the maximum spacing most commonly occurs behind the fourth axle, and that the second largest spacing most commonly occurs behind the first axle.

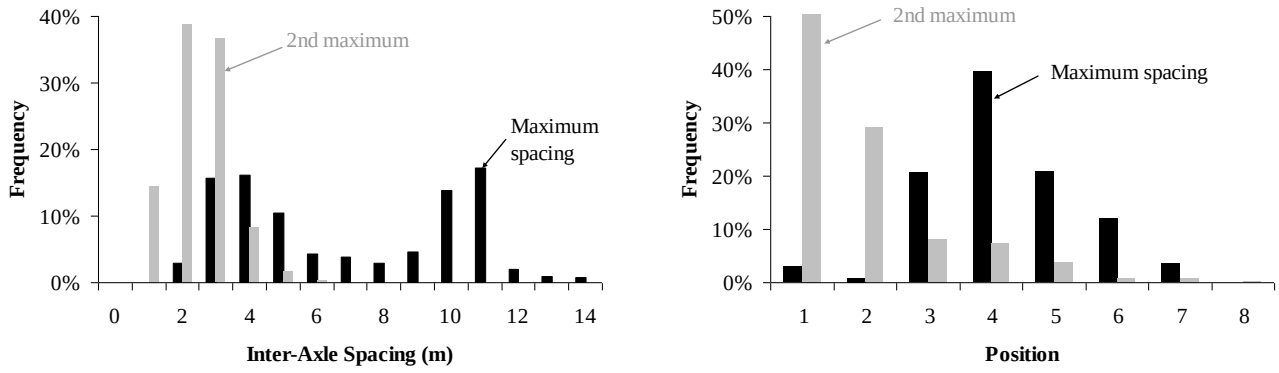

(a) Magnitude (b) Position

Fig. 3. Magnitude and position of the two largest axle spacings for all 9-axle trucks in the Netherlands.

This approach can be extended to characterize the axle layout for any vehicle. For maximum accuracy, the distributions for the magnitude and position of the first, second, third and fourth largest axle spacings in each class of vehicle are used in the simulation model. The fifth and subsequent spacings are typically in the range 1.3 m to 1.7 m, and are all modeled with a single distribution for each vehicle class. For vehicles with fewer than six axles, a reduced number of distributions is required – for example, 3-axle vehicles are completely described by the first and second largest spacing. The importance of correctly modeling axle spacing and layout is illustrated in Fig. 4 which shows the differences between the load effects on bridges of various spans for the two vehicles pictured in Fig. 2. Although these two vehicles have very similar GVWs, the shorter vehicle of Fig. 2(a) causes up to 50% greater bending moments in short to medium span simply

supported bridges, and up to 40% greater shear forces. The longer vehicle, on the other hand, causes up to 15% greater hogging moments over the central support of two-span continuous bridges. Some of these differences are caused by variations in axle loading between the two vehicles, but most of the differences can be attributed to the difference in the maximum axle spacing.

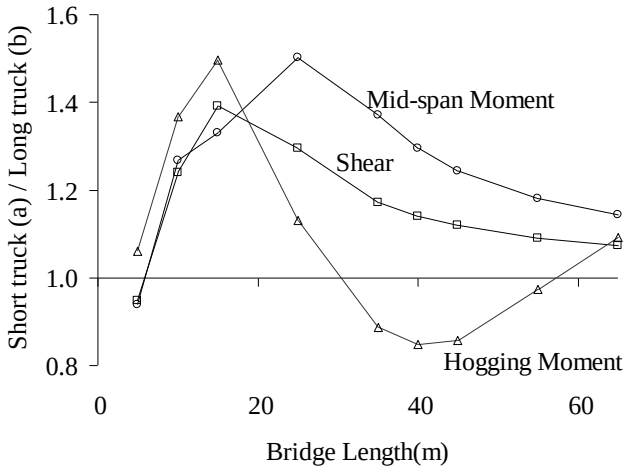

Fig. 4. Ratios of bridge load effects for the two vehicles pictured in Fig. 2.

Many different approaches have been used in modeling the distribution of the gross weight to the individual axles. Grave et al. [32], Harman and Davenport [33] and Jacob [34] use deterministic values for the proportion of GVW carried per axle for each vehicle class. Bailey and Bez [20] use bimodal beta distributions for axle groups (tandems and tridems), and Normal distributions for single axles. O'Brien et al. [21] use a mixture of Normal, bimodal Normal and trimodal Normal distributions, whereas Miao and Chan [19] use a mixture of Inverse Gaussian, Gumbel and Weibull distributions. Correlation between axle loads is modeled for each vehicle class by Crespo-Minguillón and Casas [28], and by Srinivas et al. [40] who use copula functions. The proportion of the GVW carried by each individual axle is simulated in this work by using bimodal Normal distributions fitted to the observed data for each axle from each vehicle class. An example of the fitted parameters is given in Table 6. The measured weights of adjacent axles are highly correlated, with coefficients of correlation typically in excess of 90% for closely-spaced axles, while the weights of non-adjacent axles show lower levels of correlation – typically around 50% to 60%. The observed correlation structure for both adjacent and non-adjacent axles for each vehicle class is

achieved in the simulation using the general technique for simulating correlation as described by Iman and Conover [42]. When all axle loads have been generated for a particular vehicle, their sum is generally close, but not exactly equal, to the GVW. To account for this, each axle load is scaled pro-rata to ensure that their sum is equal to the GVW. A minimum value of 25% of the average axle load for the vehicle, and a maximum value of twice the average is imposed to prevent unrealistic values being generated in the simulation. These are based on observed maxima and minima. An examination of the bridge loading scenarios that produce daily and yearly maximum load effects also ensures that these are not unduly influenced by vehicles with unusually heavy axle loads.

Table 6. Parameters of sample bimodal Normal distributions for axle loads (6-axle trucks, Czech Republic)

Axle	μ_1	σ_1	p_1	μ_2	σ_2	p_2
1	15.9%	1.8%	42.0%	22.4%	6.0%	58.0%
2	18.6%	10.4%	4.7%	18.6%	5.6%	95.3%
3	17.9%	4.0%	98.3%	24.2%	14.5%	1.7%
4	15.4%	3.0%	98.7%	24.1%	14.9%	1.3%
5	14.1%	3.6%	99.9%	43.3%	12.1%	0.1%
6	14.1%	3.7%	99.9%	33.9%	4.1%	0.1%

3.2. Extrapolated vehicle classes

As noted earlier, many authors have used models where all simulated vehicles are drawn from a fixed number of observed classes, but the model used here generates vehicles that may have more axles than any observed vehicle. The determination of the axle spacing and loading for these is based on extrapolation from observed vehicle classes. This extrapolation for all sites is based on the Dutch WIM data where the maximum number of axles observed for any vehicle is 13. At the other sites where the maximum number of axles observed is lower, the trends for axle configuration appear to be similar to comparable Dutch data. Fig. 5(a) shows the relationship between GVW and average maximum axle spacing for all countries. As GVW increases above 60 t, the data become more sparse, but the trend is similar in all countries. Fig. 5(b) shows the percentage of low loaders, defined here as those with maximum axle spacing greater than 7.5 m, as a function of GVW. In all countries, the percentage of low loaders rises steeply as GVW increases above 50 t, to approximately 50% at 100 t. In the Netherlands, the trend continues upwards to 100% for the

heaviest observed vehicles, and this clear trend in the Dutch data is assumed to be reasonable for all sites. The extreme Dutch vehicles in excess of 100 t are therefore used as a template for axle configuration for other sites, although the extrapolation of GVW is done separately for each site, based on the measured data. The graphs in Fig. 5 clearly show that there is a dependence between axle spacing and GVW.

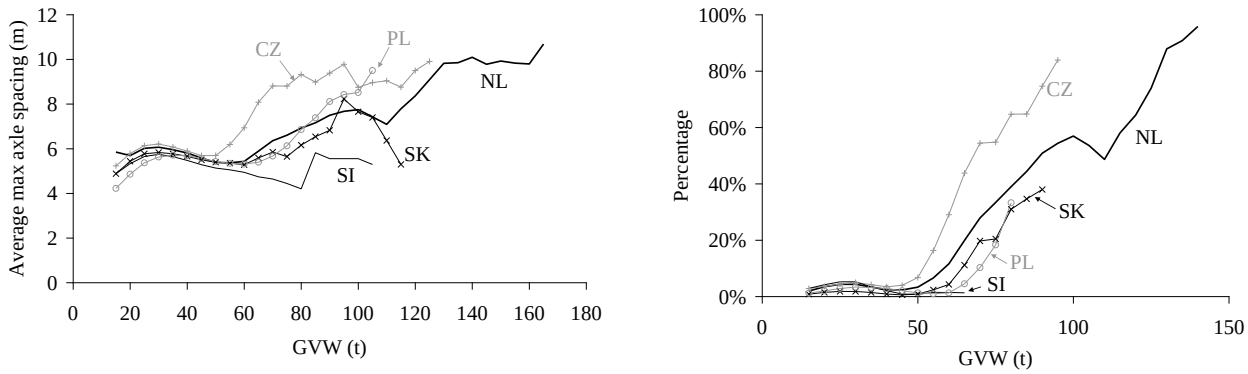

(a) Average maximum axle spacing

(b) Percentage of vehicles with maximum axle spacing over 7.5 m (“low loaders”)

Fig. 5. Trends in maximum axle spacing with weight (GVW in 1 t intervals).

The magnitude and position of all axle spacings for extrapolated vehicle classes are modeled using trimodal Normal distributions fitted to measurements for Dutch trucks with nine or more axles. Axle loading is modeled using a Normal distribution for each axle, based on the average distribution of axle loads for Dutch trucks with nine or more axles. To allow for the varying number of axles in the observed data (i.e. from 9 to 13), the random variable used for each axle is the percentage of the GVW carried by that axle divided by the average percentage per axle (e.g., (12%)/(10%) = 1.2). The percentage of the GVW carried by each of the front four axles tends to show the greatest variability, with the axles to the rear carrying similar loads.

3.3. Gaps, traffic flows and speeds

O'Brien and Caprani [42] describe the many approaches that have been used in other studies for modeling headways (the time between the front axles of successive vehicles arriving at the same point on the road). Distributions that have been used include the negative exponential, uniform, gamma, and lognormal, while some authors have used deterministic gaps. Driver behavior is influenced by the clear gap (bumper to bumper) in front of the vehicle. It is not possible to calculate

this clear gap from the available WIM data, but it is possible to calculate the inter-axle gap – the gap between the rear axle of the leading truck and the front axle of the following truck. Although headway has been used in other studies, inter-axle gap is used here as it is a better proxy for the clear gap and is not dependent on overall vehicle length. Gap distributions for each lane are fitted to the observed data for different flow rates in approximately 20 increments up to the maximum observed flow rate in each lane. For each flow rate, three piecewise quadratic curves are fitted to the observed cumulative distributions of gaps up to 4 seconds, in a similar way to that described by O'Brien and Caprani [42] for headways. For gaps greater than 4 seconds (in which case following trucks are unlikely to be on the bridge simultaneously), a negative exponential distribution is adopted as a sufficiently accurate approximation.

In other studies, traffic flow has been modeled as constant throughout the day [20], or by using "homogeneous" days with variable hourly flow which is the same for all days [25,35]. The latter approach is extended here to allow for variable daily flows which incorporate both random daily variation and any seasonal variation in the measured data. The Weibull distribution has been used elsewhere to model the temporal variation in traffic flows [43], and it gives a very good fit for the measured daily traffic volumes at all sites. The Weibull distribution parameters for each site are given in Table 7. They are used to generate a variable number of trucks for each day of the simulation. The Weibull distribution has an upper bound, and in the slow lane in the Netherlands for example, it produces daily flow values of between 4800 and 7300 trucks per day, with a mean of 6545. The Weibull distribution for maxima is given by Castillo [27]:

$$F(x;\mu,\sigma) = \exp\left\{-\left[-\left(\frac{x-\mu}{\sigma}\right)\right]^{k}\right\} \qquad (2)$$

where μ = Location, σ = Scale, $k > 0$ = Shape.

Table 7. Weibull distribution parameters for daily truck flow rates

Site	μ	σ	k
Netherlands	7 296	844	1.77
Slovakia	1 562	440	3.07
Czech Republic	6 410	2 170	2.15
Slovenia	4 067	1 027	2.15
Poland	4 187	539	1.75

The averages of the observed hourly flows throughout the 24 hour period over all measured weekdays are scaled to produce the required flow for each simulated day. The use of a variable number of trucks per day has a slight effect on the extreme value distribution of daily maxima, but when yearly maxima are used, the block size becomes effectively constant, as is required for the application of extreme value statistics. A year's traffic is assumed to consist of 250 weekdays, with the very much lighter weekend and holiday traffic being ignored. This is similar to the approach used by Caprani et al. [25] and Cooper [35]. No growth in traffic volumes is allowed for – annual average traffic flow is assumed to remain constant over the period represented by the simulation. Any seasonal variation in GVW or vehicle types is not incorporated in the model.

Truck speeds are generated using the empirical frequency distribution for each lane combined with the method described by Iman and Conover [41] to give the high correlation observed between speeds of successive vehicles. The empirical cumulative distribution for each lane at each site is calculated from the histogram of speeds in 1 km/h bins for all measured vehicles. The frequencies in the empirical distribution are re-scaled linearly to the interval (0,1), and a vehicle's speed is simulated by generating a uniform random number on this interval and selecting the corresponding speed from the empirical distribution.

The measurements at the site in Slovakia are for two lanes in opposing directions, whereas at all other sites they are for two same-direction lanes. In Slovakia, it is possible to compare directly results for simulated and observed bi-directional traffic. For the purposes of comparing simulated and observed results at the other sites, the two lanes are treated separately.

3.4. Simulation of bridge loading

The simulated traffic is passed in time steps of 0.02 s over simply supported and two-span continuous bridges of various length. Maximum load effects are calculated for each simulated loading event, and these events are categorized into different types depending on the number of trucks on the bridge in each lane when the maximum occurs. For example, in two-lane traffic there are three possible types of two-truck events – one truck in each lane, two trucks in lane 1, and two trucks in lane 2. Depending on the length of the simulation run, daily, monthly or yearly maxima are calculated for each event type. The classification of different event types has been found to improve the convergence of the results to the Generalized Extreme Value distribution [25], although this convergence also improves greatly when yearly rather than daily maxima are used. For the purposes of comparing simulated and observed results, the bridge is assumed to be a simple beam, and the transverse position of the vehicles is ignored. When estimating lifetime maximum loading, lane factors are used to model lateral distribution of axle loads.

Flowcharts for the entire simulation process are shown in Fig. 6, which shows an overview, and in Fig. 7 which shows the steps involved in generating a stream of simulated traffic (Fig. 7(a)), and the steps for calculating periodic load effect maxima produced by passing a stream of traffic over a bridge (Fig. 7(b)).

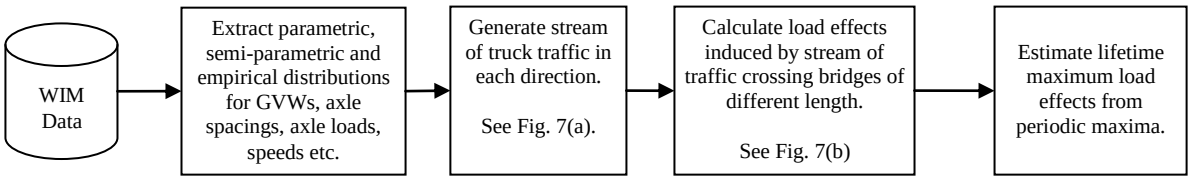

Fig. 6. Overview of simulation process

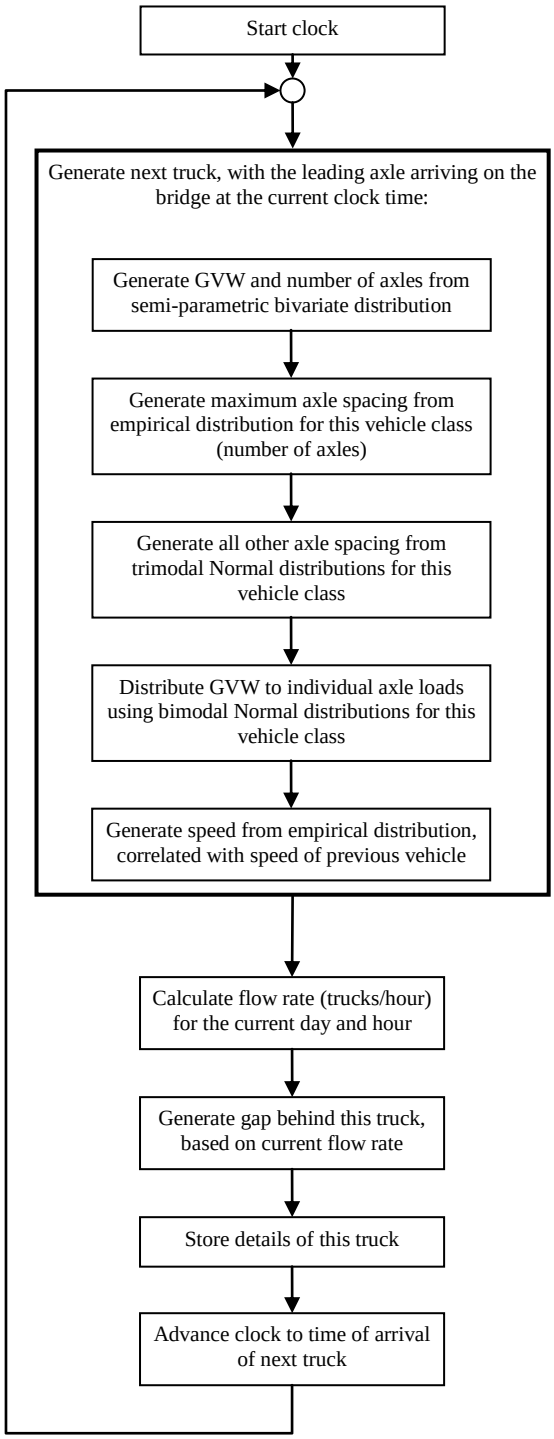

(a) Process to generate a stream of simulated truck traffic in one lane

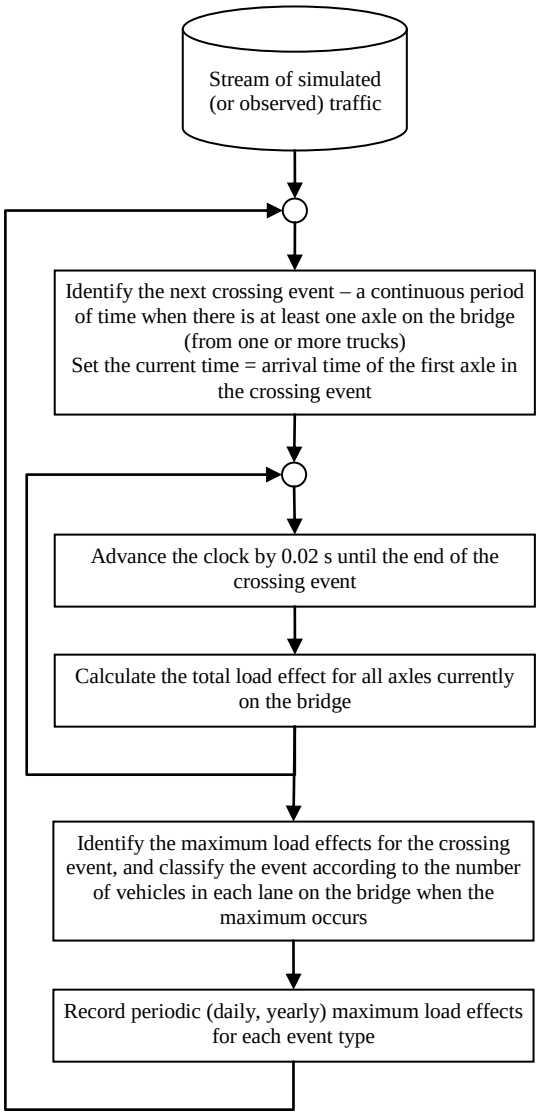

(b) Calculation of bridge load effects for a stream of truck traffic

Fig. 7. Flowcharts for simulation processes

3.5. Calibration of simulation model

The simulations are run for a time-span of 8 years (2000 working days) and the daily maximum load effects are compared with those calculated from measured traffic at each site. If observations of a random variable, drawn independently from the same parent distribution, are grouped in blocks of fixed size, the distribution of the block maxima will tend asymptotically to a Generalized Extreme Value (GEV) distribution, and a convenient way of presenting such results is to plot the calculated block maxima on Gumbel probability paper [44]. Representative results are shown in Fig. 8 and Fig. 9 for different load effects on a 35 m bridge. For the Netherlands (Fig. 8), the three loading event types shown for the slow lane are those featuring one, two and three following trucks in the same lane. The 3-truck event is relatively rare for shorter spans and does not occur on every day. This accounts for the many zero values shown for this curve. The one-truck event clearly governs over the simulated 8-year time span for both load effects.

For the bi-directional traffic in Slovakia in Fig. 9, four event types are shown – the one and two-truck same-lane events (denoted by "1" and "2" respectively), the two-truck meeting event, with a truck in each lane ("1+1"), and the three-truck meeting event, with two trucks in one lane ("2+1"). In this example, it is less clear which event type governs bridge loading over this time span, with both the one-truck and the two-truck meeting events producing similar maximum values.

Results for load effects from the simulation show good agreement with those calculated from measured data. The slight divergence of some of the measured values at the upper end of the curves can be attributed to the random nature of extreme events (as is evident in repeated simulation runs, for example), and the principal objective of the simulation is to ensure that the model matches the main trends in the observed data.

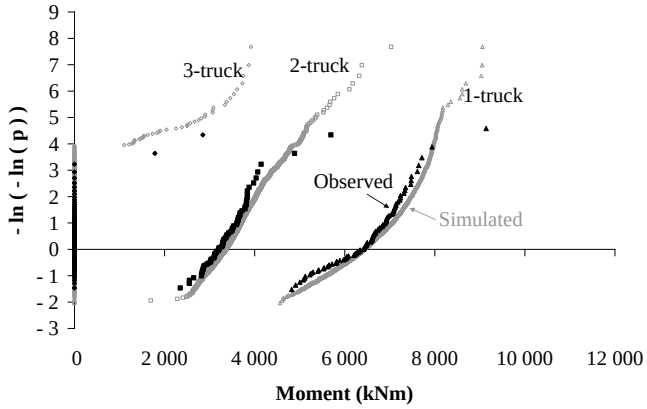

(a) Mid-span moment, simply supported

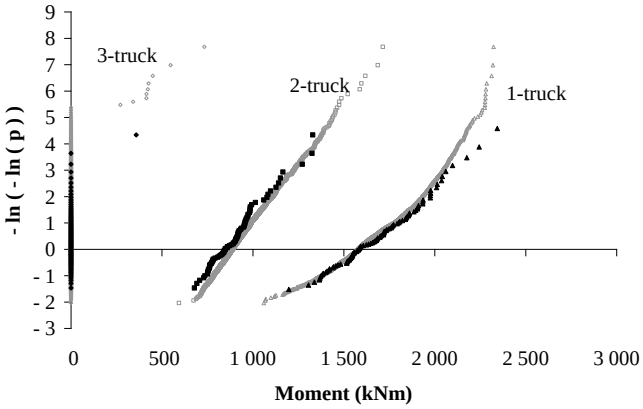

(b) Mid-support hogging moment, 2-span continuous bridge

Fig. 8. The Netherlands, slow lane only: Daily maximum load effects, bridge length = 35 m

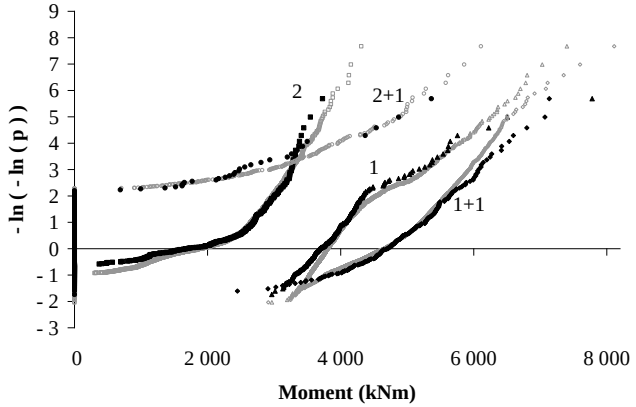

(a) Mid-span moment, simply supported

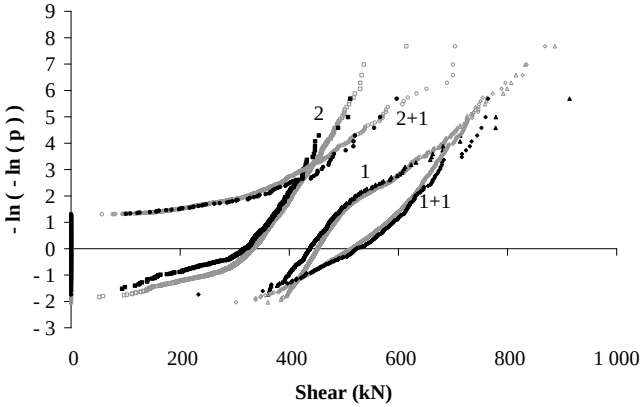

(b) Support Shear, simply supported

Fig. 9. Slovakia, bi-directional traffic: Daily maximum load effects, bridge length = 35 m

4. USING THE SIMULATION MODEL TO ESTIMATE MAXIMUM LIFETIME LOADING

4.1. Modeling two-lane traffic

The traffic modeled for this study is bidirectional, with one lane in each direction, and independent streams of traffic are generated for each direction. In simulation, many millions of loading events

are analyzed, and for efficiency of computation it is necessary to use a reasonably simple model for transverse load distribution on two-lane bridges. This is achieved by calculating load effects for each vehicle based on a simple beam, and multiplying these load effects by a lane factor to account for transverse distribution. The lane factors used are based on finite element analyses which were performed on bridges with different spans (from 12 to 45 m), and different construction methods (solid slab for shorter spans, and beam-and-slab for longer spans). One lane is identified as the "primary" lane and the lane factor for vehicles in this lane is always taken as unity. When a vehicle is also present in the other "secondary" lane, the location of maximum stress is identified in the finite element model, and the relative contributions of each truck is calculated. In some cases the maximum stress occurs in a central beam, and the contribution from each truck is similar, giving a lane factor close to 1.0 for the secondary lane. In other cases, the maximum stress occurs in a beam under the primary lane, and the lane factor for the secondary lane is significantly reduced. In the case of shear stress at the supports of a simply supported bridge, the maximum occurs when each truck is close to the support, and the lateral distribution is very much less than for mid-span bending moment. As a result of this analysis, two sets of lane factors are used in the simulation runs, one at either end of the calculated ranges – "low" and "high". The factors used are shown in Table 8, together with the three types of load effect that are examined in all simulation runs.

Table 8. Lane Factors for secondary lane

	Load Effect	**Lane Factors**	
		Low	**High**
LE1	Mid-span bending moment, simply supported	0.45	1.0
LE2	Support shear, simply supported	0.05	0.45
LE3	Central support hogging moment, 2-span continuous	0.45	1.0

At the WIM sites in four of the five countries, the data are for two same-direction lanes, and the percentage of the total truck traffic in the slow lane ranges between 92% and 96%. For the purposes of this study, the truck volumes in the faster lane are merged with the slow lane to give a stream of single-lane traffic, with gap distributions adjusted for the slightly higher flow rate. This is similar to the approach that has been used in other studies [24] and is conservative as it neglects the increased gaps between trucks that would be introduced by merging all traffic – trucks and cars – in both

lanes. In Slovakia, where the measurements are for the slow lane only in each direction, the simulation is based on the measured traffic flows. According to Rogers [45], the peak capacity of a two-lane bidirectional road is approximately 2000 vehicles per hour in each lane, and while the percentage of trucks is site dependent it would typically be in the range of 5% to 15%. This would imply that the truck volumes in the Netherlands would most likely cause congestion, but that the volumes at the other sites could quite plausibly be carried by a two-lane bridge. The WIM data from the Netherlands are very useful in characterizing the axle configuration for extremely heavy vehicles in all countries, but the bridge loading results presented here are confined to the four Central European countries.

The programs which implement the simulation model are written in C++, and use parallel processing. Only potentially significant crossing events are examined in detail – i.e. where the combined GVW on the bridge exceeds a selected threshold. This is a form of importance sampling [46,47] and greatly reduces the required processing time. For example, at the Czech site where the traffic volume is relatively high (4751 trucks per day in each direction), there are 2.4×10^9 vehicles in 1000 years of bidirectional traffic. Using the programs designed by the authors, a full simulation of these events and calculation of load effects for four bridge spans takes about 4 days on a single personal computer with a 1.73 GHz Intel® Pentium® Dual-Core processor. By focussing on only significant crossing events, the processing time can be reduced to about 1 day.

4.2. Results from 1000-year simulation runs

1000-year simulations were performed for each site. The simulated traffic was run over four bridge lengths – 15, 25, 35 and 45 m – and three load effects were calculated for low and high transverse distribution (lane factors), as shown in Table 8.

The output from each simulation run includes the annual maximum value of each load effect for each of the event types described earlier, as well as the overall annual maximum load effect, regardless of event type. These can be plotted on Gumbel probability paper as shown for example in Fig. 10 for mid-span bending moment on a simply supported 35 m bridge with low transverse distribution. A Weibull fit to the top 30% of values is also shown. As can be seen, the fit for the Czech data is almost linear, suggesting a Gumbel distribution, whereas for the other sites there is more pronounced curvature, indicating that the Weibull distribution is more appropriate. The traffic

volumes vary significantly between sites, and consequently the number of loading events per year is quite different. The GVW distribution is also different at each site. These two factors are considered to explain the differences in the distributions of load effects at each site. An advantage of using the Weibull distribution is that it encompasses the Gumbel distribution as the limiting case as the shape factor tends towards zero.

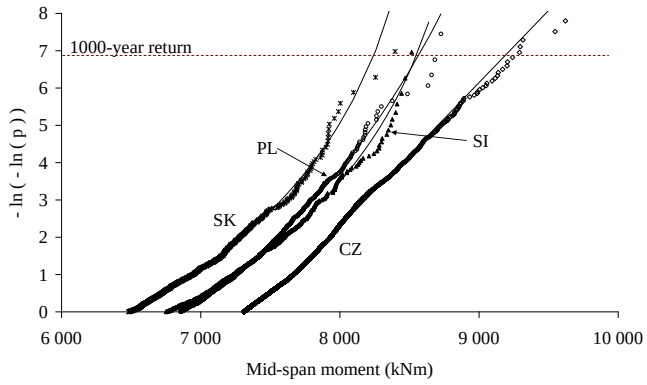

Fig. 10. Load Effect 1, low lane factors, 35 m span, overall annual maxima, with Weibull fits to top 30% (SK = Slovakia, PL = Poland, CZ = Czech Republic, SI = Slovenia)

In Table 9, sample results for lifetime maximum loading are given for a 35 m bridge. It can be seen that the 50-year and 75-year mean values are very similar in magnitude, and are approximately 10% lower than the 1000-year return values. The COV of the 50 and 75 year mean values are around 5%, and this compares with other studies of site-specific static load effects – for example, Moses [5] cites reported results from various studies of between 1% and 5% for maximum loading events. Repeated simulation runs will give slightly different estimates, but the variance between runs is quite small – for example, the estimate for the 75-year mean has a COV of about 1.0%.

In Fig. 11, some sample schematic layouts of maximum-in-lifetime loading scenarios are shown. For each site, bridge span, load effect and level of transverse distribution, similar diagrams are generated for the top 20 loading events in 1000 years of simulation. These are useful in assessing the plausibility of the estimated characteristic values, and an analysis of these scenarios allows some conclusions to be drawn about the types of vehicles and loading events that are likely to cause the maximum loading in the lifetime of the bridge. These conclusions are summarized for each load effect in the following paragraphs.

Table 9. Characteristic maximum load effects – 35 m bridge

Site	Lane Factors	1000-year return value	50-Year Mean	50-year COV	75-Year Mean	75-year COV
LE1: Mid-span Moment (kNm)						
Czech Republic	High	10 766	9 853	4.9%	9 994	4.6%
	Low	9 539	8 592	5.2%	8 699	5.4%
Slovenia	High	10 548	9 383	6.2%	9 498	6.1%
	Low	8 905	8 220	4.4%	8 288	4.5%
Poland	High	10 202	9 441	4.7%	9 563	4.7%
	Low	8 631	8 136	3.3%	8 227	3.3%
Slovakia	High	9 862	8 776	6.9%	8 933	6.9%
	Low	8 368	7 864	3.5%	7 914	3.5%
LE2: Support shear (kN)						
Czech Republic	High	1 177	1 058	5.6%	1 073	5.6%
	Low	1 165	1 049	5.6%	1 061	5.5%
Slovenia	High	1 088	989	5.9%	1 005	6.1%
	Low	1 087	983	6.3%	998	6.6%
Poland	High	1 059	978	4.4%	988	4.4%
	Low	1 049	967	4.3%	978	4.3%
Slovakia	High	1 003	935	3.9%	945	3.9%
	Low	992	934	3.6%	945	3.6%
LE3: Hogging Moment [a]- Central Support (kNm)						
Czech Republic	High	2 687	2 439	5.3%	2 474	5.2%
	Low	2 489	2 279	4.9%	2 312	4.7%
Slovenia	High	2 569	2 270	7.2%	2 309	7.2%
	Low	2 428	2 115	7.7%	2 162	7.6%
Poland	High	2 459	2 254	5.2%	2 291	5.1%
	Low	2 263	2 092	4.6%	2 118	4.4%
Slovakia	High	2 312	2 091	5.6%	2 122	5.4%
	Low	2 235	2 057	4.9%	2 090	4.5%

Note: [a] For hogging moment, the results are for a 2-span bridge with an overall length of 35 m.

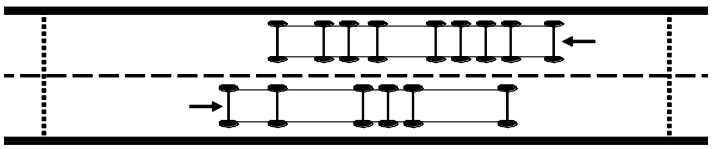

(a) Czech Republic, high lateral distribution
Load effect 1: Mid-span moment, simply supported
104 t and 61 t

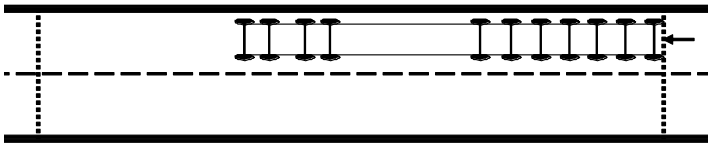

(b) Poland, low lateral distribution
Load effect 2: Support shear, simply supported
157 t

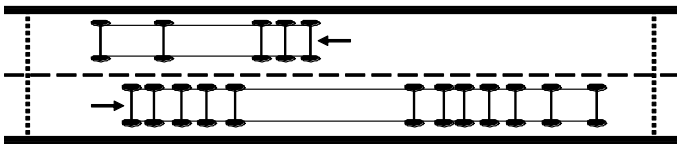

(c) Slovenia, high lateral distribution
Load effect 3: Hogging moment, two-span
33 t and 148 t

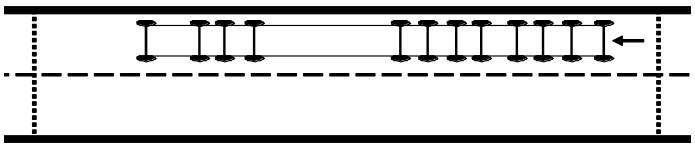

(d) Slovakia, low lateral distribution
Load effect 3: Hogging moment, two-span
165 t

Fig. 11. Schematics of selected maximum-in-lifetime loading scenarios on a 35 m bridge

Load Effect 1 – Mid-span bending moment, simply supported

Where there is high transverse distribution of load, typical lifetime maximum loading events feature two trucks meeting on the bridge. In most cases, there is one very heavy vehicle meeting a more frequent 5 or 6-axle truck, as in Fig. 11(a) for the Czech Republic. This is an example of Turkstra's rule [48]. The heavy vehicle is typically a crane-type vehicle with closely-spaced axles and a GVW within the range observed in the WIM data. When there is low transverse distribution, 1-truck

events are more common and often feature a heavy crane or a low loader significantly heavier than any observed. Two-truck events still feature, although usually with one very heavy truck meeting a frequent truck.

Load Effects 2 – Shear at support, simply supported

For shear, transverse distribution is relatively low (see Table 8) because the trucks are close to the bridge abutments. As a consequence, one-truck events tend to dominate, often composed of a low loader significantly heavier than any observed vehicle, as in Fig. 11(b) for Poland. In some cases, there is a light truck on the bridge at the same time. Due to the assumptions in the simulation based on WIM data from the Netherlands, low loaders are the dominant type for the heaviest vehicles.

Load Effect 3 – Hogging moment over central support, two-span continuous bridge

Low loaders also feature frequently for this load effect, partly because they are the dominant type above 120 t, but also because of the shape of the influence line for hogging bending moment. A low loader can straddle both spans and so produce higher moments than a crane-type vehicle of the same GVW. Some events have a heavy low loader in one lane meeting a frequent truck in the other lane, as in Fig. 11(c) for Slovenia. For low transverse distribution, one-truck events are more common and the single truck tends to have a GVW significantly heavier than any observed as in Fig. 11(d) for Slovakia.

5. CONCLUSIONS

Extensive collections of high-quality WIM measurements have been used to calibrate a bridge traffic loading model which seeks to capture all significant aspects of heavy vehicle traffic. The measurements are considered to be typical of traffic on European highways in recent years. The model is site-specific in that each simulation run is based on statistical distributions of parameters measured at a particular location, but can be used for any site where WIM measurements are available. The simulated results for load effects are shown to match those for measured data. The model can be used to estimate maximum bridge load effects over a chosen time span and can be used either in the assessment of existing bridges or for the verification and re-calibration of bridge

design or assessment codes. The model is designed to extrapolate in a consistent way from measured traffic to vehicles that are heavier and have more axles than any that have been observed.

Results are dependent on the method chosen for extrapolating measured GVWs to estimate lifetime maximum weights, and on the assumptions used in generating vehicles with a greater number of axles than any observed in the WIM data. The results are particularly sensitive to the modeling assumptions regarding axle spacings and wheelbase. Results for loading events which feature two or more trucks in the same lane are sensitive to the modeling of inter-vehicle gaps. If vehicles are simulated to travel more closely together, there is a higher probability of a greater concentration of load on the bridge. However, this type of loading event has not been found to be critical in the lifetime of the bridge spans considered.

Previous approaches using Monte Carlo simulation have required many simplifying assumptions. The model described here aims to remove as many limitations as possible and to develop a simulation model that is generally applicable to many different vehicle types. While design and assessment codes usually separate special vehicles requiring permits from normal traffic, the model presented here includes the entire population of highway-speed vehicles that a bridge is likely to carry during its lifetime.

The simulation process has been optimized to allow very long runs to be done, in excess of 1000 years, and this greatly reduces the variability of results and largely avoids issues about the selection of suitable statistical distributions for extrapolation from short simulation runs. Estimates with low variance can be calculated for characteristic 1000-year load effects and for the distributions of 50- and 75-year lifetime maxima that can be used for reliability-based design and assessment. The approach described here does not remove the uncertainty inherent in estimating lifetime maximum loading from data collected over time periods which are much shorter than the bridge lifetime.

The long-run simulations make it possible to examine in detail the types of loading events that give rise to the characteristic load effects. Bridge loading for the spans considered at these sites is governed by single-truck and 2-truck meeting events. The 1-truck events often feature trucks significantly heavier than any observed. The 2-truck events generally feature an extremely heavy truck meeting an average truck (Turkstra’s rule), with the weight of the heavy truck often within the range of the observed data.

In general, special vehicles well above normal legal weight limits govern bridge loading. For bridge owners, the monitoring and control of these "special" vehicles is essential. Reducing the frequency of crane-type vehicles would reduce the probability of these meeting other heavy trucks on a bridge. Extremely heavy low loaders are rarer at all sites, but controlling the gross weight of these would also reduce the characteristic maximum-in-lifetime loading.

6. ACKNOWLEDGEMENTS

The authors gratefully acknowledge the support of DVS in the Dutch Ministry of Transport and Waterworks, and of the 6th Framework European Project, ARCHES.

7. REFERENCES

[1] Jacob, B. and O'Brien, E. J. Weigh-In-Motion: Recent developments in Europe. In: E. J. O'Brien, B. Jacob, A. González, and C.-P. Chou, eds. Fourth International Conference on Weigh-In-Motion (ICWIM4), Taipei, Taiwan: National Taiwan University; 2005.

[2] EC1. Eurocode 1: Actions on structures, Part 2: Traffic loads on bridges. Brussels: European Standard EN 1991-2:2003: European Committee for Standardization, TC250; 2003.

[3] Flint, A. R. and Jacob, B. Extreme Traffic Loads on Road Bridges and Target Values of Their Effects for Code Calibration. Proceedings of IABSE Colloquium, Delft, The Netherlands: IABSE-AIPC-IVBH; 1996, 469 - 78.

[4] Kulicki, J. M., Prucz, Z., Clancy, C. M., Mertz, D. and Nowak, A. S. Updating the calibration report for AASHTO LRFD code: NCHRP. Washington D.C.: Transportation Research Board; 2007.

[5] Moses, F. Calibration of load factors for LRFR Bridge Evaluation: NCHRP Report No. 454. Washington D.C.: Transportation Research Board; 2001.

[6] O'Connor, A. and Enevoldsen, I. Probability-based assessment of highway bridges according to the new Danish guideline. Structure and Infrastructure Engineering 2009; 5 (2): 157-68.

[7] Laman, J. A. and Nowak, A. S. Site-specific truck loads on bridges and roads. Proceedings of ICE, Transport 1997; 1997, 123 (May): 119-33.

[8] Park, M.-S., Park, C.-H. and Lee, J. Development of local live load truck model for long span bridges based on BWIM data of Seohae cable-stayed bridge. In: H.-M. Koh and D. M. Frangopol, eds. Fourth International Conference on Bridge Maintenance, Safety, Management, Health Monitoring and Informatics, Seoul, Korea: Taylor & Francis Group, London; 2008.

[9] Sivakumar, B. and Ibrahim, F. I. S. Enhancement of bridge live loads using weigh-in-motion data. Bridge Structures 2007; 3 (3-4): 193-204.

[10] Nowak, A. S. Live load model for highway bridges. Structural Safety 1993; 13: 53-66.

[11] Nowak, A. S. Load model for bridge design code. Canadian Journal of Civil Engineering 1994; 21: 36-49.
[12] Dawe, P. Research Perspectives: Traffic loading on highway bridges. London: Thomas Telford; 2003.
[13] O'Connor, A., Jacob, B., O'Brien, E. J. and Prat, M. Report of current studies performed on normal load model of EC1 Part 2. Traffic loads on bridges. Revue Française de Génie Civil 2001; 5 (4): 411-33.
[14] European Commission and Eurostat. Energy and transport in figures - Part 3: Transport: European Commission; 2007.
[15] Minervino, C., Sivakumar, B., Moses, F., Mertz, D. and Edberg, W. New AASHTO Guide Manual for Load and Resistance Factor Rating of Highway Bridges. Journal of Bridge Engineering, ASCE 2004; 9 (1): 43-54.
[16] Sivakumar, B., Moses, F., Fu, G. and Ghosn, M. Legal truck loads and AASHTO Legal Loads for Posting: NCHRP Report 575; 2007.
[17] Nowak, A. S., Nassif, H. H. and DeFrain, L. Effect Of Truck Loads On Bridges. Journal of Transportation Engineering (ASCE) 1993; 119 (6): 853-67.
[18] Vrouwenvelder, A. C. W. M. and Waarts, P. H. Traffic Loads on Bridges. Structural Engineering International 1993; 3 (3): 169-77.
[19] Miao, T. J. and Chan, T. H. T. Bridge live load models from WIM data. Engineering Structures 2002; 24: 1071-84.
[20] Bailey, S. F. and Bez, R. Site specific probability distribution of extreme traffic action effects. Probabilistic Engineering Mechanics 1999; 14: 19-26.
[21] O'Brien, E. J., Caprani, C. C. and O'Connell, G. J. Bridge assessment loading: a comparison of West and Central/East Europe. Bridge Structures 2006; 2 (1): 25-33.
[22] O'Connor, A. and O'Brien, E. J. Traffic Load Modelling and Factors Influencing the Accuracy of Predicted Extremes. Canadian Journal of Civil Engineering 2005; 32 (1): 270 - 8.
[23] Gindy, M. and Nassif, H. H., Comparison of traffic load models based on simulation and measured data. Joint International Conference on Computing and Decision Making in Civil and Building Engineering, Montréal, Canada; 2006, [online] available from: http://www.icccbexi.ca/html/en/AutIndex.htm#G, accessed 8 May 2007
[24] Cooper, D. I. Development of short-span bridge-specific assessment live loading. in Safety of bridges, P. C. Das, ed., Thomas Telford, London; 1997 64-89.
[25] Caprani, C. C., O'Brien, E. J. and McLachlan, G. J. Characteristic traffic load effects from a mixture of loading events on short to medium span bridges. Structural Safety 2008; 30 (5): 394-404, doi: 10.1016/j.strusafe.2006.11.006.
[26] James, G. Analysis of traffic load effects on railway bridges using weigh-in-motion data. In: E. J. O'Brien, B. Jacob, A. González, and C.-P. Chou, eds. Fourth International Conference on Weigh-In-Motion (ICWIM4), Taipei, Taiwan: National Taiwan University; 2005.
[27] Castillo, E. Extreme value theory in engineering. Boston: Academic Press; 1988.
[28] Crespo-Minguillón, C. and Casas, J. R. A comprehensive traffic load model for bridge safety checking. Structural Safety 1997; 19 (4): 339-59.
[29] Cremona, C. Optimal extrapolation of traffic load effects. Structural Safety 2001; 23: 31-46.
[30] Buckland, P. G., Navin, F. P. D., Zidek, J. V. and McBryde, J. P. Proposed vehicle loading of long-span bridges. Journal of the Structural Division, ASCE 1980; 106 (No. ST4): 915-32.

[31] Ghosn, M. and Moses, F. Reliability calibration of bridge design code. Journal of Structural Engineering, ASCE 1986; 112 (4): 745-63.
[32] Grave, S. A. J., O'Brien, E. J. and O'Connor, A. J. The determination of site-specific imposed traffic loadings on existing bridges. in Bridge Management 4, M. J. Ryall, G. A. R. Parke, and J. E. Harding, eds., Thomas Telford, London; 2000 442-9.
[33] Harman, D. J. and Davenport, A. G. A statistical approach to traffic loading on highway bridges. Canadian Journal of Civil Engineering 1979; 6: 494-513.
[34] Jacob, B. Methods for the prediction of extreme vehicular loads and load effects on bridges. Report of Subgroup 8, Eurocode 1 1991.
[35] Cooper, D. I. The determination of highway bridge design loading in the United Kingdom from traffic measurements. In: Jacob B. et al., ed. First European Conference on Weigh-in-Motion of Road Vehicles, ETH, Zurich; 1995, 413-21.
[36] Kennedy, D. J. L., Gagnon, D. P., Allen, D. E. and MacGregor, J. G. Canadian highway bridge evaluation: load and resistance factors. Canadian Journal of Civil Engineering 1992; 19: 992-1006.
[37] OBrien, E. J., Enright, B. and Getachew, A. Importance of the Tail in Truck Weight Modeling for Bridge Assessment. Journal of Bridge Engineering, ASCE 2010; 15 (2): 210-3, doi: http://dx.doi.org/10.1061/(ASCE)BE.1943-5592.0000043
[38] Tabsh, S. W. and Tabatabai, M. Live load distribution in girder bridges subject to oversized trucks. Journal of Bridge Engineering, ASCE 2001; 6 (1): 9-16.
[39] Sriramula, S., Menon, D. and Anumolu, P. M. Modeling of highway traffic for bridges in India. In: G. Augusti, G. I. Schueller, and M. Ciampoli, eds. International Conference on Structural Safety and Reliability (ICOSSAR) 2005, Rome; 2005.
[40] Srinivas, S., Menon, D. and Prasad, A. M. Multivariate Simulation and Multimodal Dependence Modeling of Vehicle Axle Weights with Copulas. Journal of Transportation Engineering (ASCE) 2006; December 2006: 945-55.
[41] Iman, R. L. and Conover, W. J. A distribution-free approach to inducing rank correlation among input variables. Communications in Statistics – Simulation and Computation 1982; 11 (3): 311 - 34.
[42] O'Brien, E. J. and Caprani, C. C. Headway modelling for traffic load assessment of short- to medium-span bridges. The Structural Engineer 2005; 83 (16): 33-6.
[43] Stathopolous, A. and Karlaftis, M. Temporal and spatial variations in real-time traffic data in urban Athens. Transportation Research Record: Journal of the Transportation Research Board 2001; 1768: 135-40.
[44] Ang, A. H.-S. and Tang, W. H. Probability concepts in engineering planning and design. New York: Wiley; 1975.
[45] Rogers, M. Highway Engineering. 2nd Edition. Oxford: Blackwell Publishing; 2008.
[46] Rubinstein, R. Y. Simulation and the Monte Carlo Method. New York: John Wiley & Sons; 1981.
[47] Townsend, J. K., Haraszti, Z., Freebersyser, J. A. and Devetsikiotis, M. Simulation of Rare Events in Communications Networks. IEEE Communications Magazine 1998; August 1998: 36-41.
[48] Naess, A. and Røyset, J. Ø. Extensions of Turkstra's rule and their application to combination of dependent load effects. Structural Safety 2000; 22: 129-43.